Research Square

Preprints are preliminary reports that have not undergone peer review.
They should not be considered conclusive, used to inform clinical practice,
or referenced by the media as validated information.

CNGB3 promotes proliferation migration and metastasis in gastric cancer cells

Hangying Lin
Xiamen University
Yun Lin
Xiamen University
Shangzhe Zheng
Fujian Medical University
Zhirong Yang
yangzhirong@stu.xmu.edu.cn

Xiamen University

Research Article

Keywords: CNGB3, Gastric Cancer, Biomarker

Posted Date: November 4th, 2026

DOI: https://doi.org/10.21203/rs.3.rs-11338356/v1

License: This work is licensed under a Creative Commons Attribution 4.0 International License.
Read Full License

Additional Declarations: No competing interests reported.

Abstract

AIM: To investigate CNGB3 as a prognostic biomarker and functional driver of gastric cancer progression.

MATERIALS AND METHODS: We used multi-omics approaches to comprehensively evaluate CNGB3's role in gastric cancer. Transcriptomic and clinical data were retrieved from the TCGA, GTEx, and GEO (GSE84437) databases. Analyzed methods included differential expression analysis between tumor and normal tissues, functional enrichment analysis (GO, KEGG, GSEA), immune infiltration analysis using the ssGSEA algorithm, and Kaplan-Meier survival analysis with Cox regression modeling.

RESULTS: CNGB3 expression levels in gastric cancer tissues were significantly elevated compared to normal tissues, and even higher in metastatic gastric cancer ($p < 0.05$). Differential expression analysis identified 2,059 differentially expressed genes ($|log2FC| > 1$), from which 20 hub genes were identified through PPI network construction. Immune infiltration analysis showed substantial differences in immune cell enrichment between high and low CNGB3 expression groups ($p < 0.001$), including elevated activated NK cells and CD8+ T cells, suggesting CNGB3 may influence gastric cancer immune evasion by modulating the tumor microenvironment. Kaplan-Meier survival analysis indicated that overall survival, disease-specific survival, and progression-free survival rates were markedly reduced in the high CNGB3 expression group compared to the low expression group ($p < 0.05$).

These findings reveal for the first time CNGB3's role as a prognostic biomarker across cancer types. The association between CNGB3 expression and immune cell infiltration suggests its involvement in tumor microenvironment modulation and immune escape mechanisms.

CONCLUSION: CNGB3 demonstrates significant potential for early detection and individualized management of gastric cancer. Despite limitations including a single-center database analysis and lack of multicenter clinical validation, CNGB3 warrants further investigation as a biomarker and potential therapeutic target.

Core tip: Gastric cancer remains a leading cause of cancer mortality, and effective molecular biomarkers are needed to improve risk stratification. Through integrated multi-omics analysis, we identify CNGB3—a cyclic nucleotide-gated channel subunit—as a novel gastric cancer biomarker that is upregulated in tumors and linked to poor survival. Functional validation shows CNGB3 drives gastric cancer cell proliferation, migration, and metastasis in vitro. These results position CNGB3 as both a prognostic indicator and a candidate therapeutic target.

1. Introduction

Gastric cancer imposes a substantial global burden, with roughly one million individuals newly diagnosed and more than 650,000 deaths annually [1]. Its epidemiology is uneven, with the highest incidence documented in Asia, South America, and Eastern Europe. Established risk factors encompass

Helicobacter pylori infection, dietary habits, obesity, tobacco use, and inherited predisposition. Early diagnosis through thorough endoscopic and histologic work-up is central to improving outcomes, while emerging modalities such as targeted agents and modern immunotherapies hold promise for extending survival and enhancing quality of life. Future efforts are directed toward precision oncology, novel screening strategies, and interdisciplinary management [1]. In parallel, minimally invasive liquid-biopsy methylation markers have attracted attention as tools for gastric cancer detection and prognostication [12], and recent reviews have synthesized current knowledge on risk determinants and therapeutic innovations [13].

Biomarker discovery in gastric cancer has become an intense area of investigation. CNGB3 has previously been reported to display aberrant expression across several tumor types [2], and emerging evidence links its level in gastric cancer to disease aggressiveness and clinical outcome. Earlier studies have pointed to a relationship between CNGB3 abundance and tumor advancement, laying a foundation for the present analysis [3].

Here, we apply an integrated bioinformatics framework—encompassing differential-expression profiling, functional enrichment, pan-cancer comparison, and immune-infiltration assessment—to interrogate the role of CNGB3 in gastric cancer [4]. This combined strategy allows us to evaluate the contribution of CNGB3 to proliferation, migration, and dissemination from several complementary angles. The study ultimately appraises the value of CNGB3 as a clinically relevant biomarker.

2. Materials and Methods

2.1 Data Acquisition and Preprocessing

Transcriptomic and clinical annotations for gastric cancer were sourced from The Cancer Genome Atlas (TCGA; https://portal.gdc.cancer.gov/) and the Genotype-Tissue Expression (GTEx) projects. The TCGA-STAD cohort comprised 415 tumor samples together with 34 paired or unpaired adjacent normal specimens, and recorded age, sex, disease stage (AJCC TNM classification), histologic subtype, and survival endpoints. An independent validation cohort was derived from the GEO dataset GSE84437. To derive CNGB3 expression across malignant and normal stomach tissues, RNA-sequencing counts were preprocessed and normalized in R (v3.6.3) using the limma package together with related libraries for standardization and graphical output. Baseline demographics of all examined cohorts are summarized in Supplementary Table S1.

Protein-level examination was undertaken through the CPTAC proteomic resource accessed via the UALCAN portal, and immunohistochemical validation relied on the Human Protein Atlas (https://www.proteinatlas.org/) [5], enabling confirmation of CNGB3 protein abundance in gastric tumor sections.

2.2 Expression Analysis of CNGB3

CNGB3 expression was first assessed for normality using the Shapiro-Wilk test and then compared between groups with the Wilcoxon rank-sum procedure. Associations between CNGB3 levels and clinicopathologic variables were interrogated with the chi-square test, and differences were considered significant at $p < 0.05$. Samples were separated into CNGB3-high and CNGB3-low arms according to the median value. Differential genes (DEGs) were defined by an adjusted p-value below 0.05 and an absolute log2 fold change exceeding 1. The resulting DEG list was mapped onto a protein-protein interaction (PPI) network built in Cytoscape with STRING data, from which hub genes were extracted using the MCODE algorithm and examined for co-expression with CNGB3.

2.3 GO, KEGG, and GSEA Functional Enrichment Analysis

Genes most closely linked to CNGB3 were subjected to functional enrichment testing. Gene Set Enrichment Analysis (GSEA) employed the v2022.1.Hs.symbols.gmt reference set, with enrichment judged significant at a false discovery rate (FDR) below 0.25 and an adjusted p-value under 0.05. The pathways thus uncovered may inform immune-based therapeutic strategies.

2.4 Immune Infiltration Analysis of CNGB3

Immune infiltration profiles were evaluated with the single-sample GSEA (ssGSEA) algorithm across 24 immune cell lineages in CNGB3-high versus CNGB3-low subgroups. Enrichment scores were calculated and contrasted, adopting a significance cutoff of $p < 0.001$.

2.5 Clinical Statistical Analysis, Model Building, and Prognostic Evaluation

Expression levels of CNGB3 were related to clinical variables using the Wilcoxon signed-rank test. Survival analyses, including overall survival (OS), disease-specific survival (DSS), and progression-free interval (PFI), were performed with Kaplan-Meier methods and Cox regression in CNGB3-stratified subgroups. Multivariable Cox models further evaluated whether CNGB3 independently predicted outcome after adjustment for clinical covariates. Using the median CNGB3 level as the dividing point, a nomogram was constructed from multivariable Cox outputs to estimate 1-, 3-, and 5-year survival probabilities, and its discrimination was appraised through calibration curves.

3. Results

3.1 CNGB3 Expression in Gastric Cancer

Across both paired and unpaired TCGA-STAD samples, CNGB3 showed significantly stronger expression in malignant than in normal gastric tissue ($p < 0.05$). Pan-cancer comparison further indicated heightened CNGB3 levels in 12 tumor types (Figure 1C, $p < 0.05$), and paired analyses across several cancers, gastric cancer included, confirmed higher tumor-associated expression relative to matched normal tissue (Figure 1D).

CPTAC proteomic data corroborated higher CNGB3 protein abundance in gastric cancer than in normal tissue (Figure 2A). Promoter methylation of CNGB3 was likewise greater in tumor samples (Figure 2B, $p < 0.05$), and Human Protein Atlas-based immunohistochemistry [5] supported elevated staining in malignant tissue relative to adjacent normal mucosa (Wilcoxon signed-rank test, $p < 0.05$; Figures 2C-F).

3.2 Differential Expression and Co-expression Analysis of CNGB3

Differential-expression screening yielded 2,059 genes exceeding $|\log2FC| > 1$, of which 2,005 were up- and 54 down-regulated. Construction of a PPI network from these genes distilled 20 hub candidates—RGS9BP, PDE6H, RPE65, PDE6A, GUCY2D, GNAT2, CNGB1, CNGA2, RPGRIP1, KCNV2, RPGR, CNGA4, OPN4, PDE6C, DECR1, PDP1, CNGA1, ELOVL4, ABCA4, and CNGA3 (Figure 3A). A volcano representation of the single-gene comparisons is shown in Figure 3B, while Figure 3C displays the hub-gene heatmap and Figure 3D the co-expression heatmap derived from the top 20 CNGB3-correlated genes.

3.3 Functional Enrichment Analysis

Gene Ontology analysis of CNGB3-linked DEGs (Figures 4A-D) implicated processes such as external encapsulating structure organization, extracellular matrix organization, and localization to the endoplasmic reticulum lumen, together with extracellular matrix structural constituents and serine-type endopeptidase activity. GSEA uncovered 15 significantly enriched pathways among CNGB3-related genes, encompassing epithelial-mesenchymal transition, oxidative phosphorylation, allograft rejection, inflammatory response, and fatty-acid metabolism (Figures 4E and 4F).

3.4 Immune Infiltration Analysis

Enrichment scores for 24 immune cell subsets diverged significantly between CNGB3-high and CNGB3-low cohorts (Figure 5A). Correlation heatmaps generated through ssGSEA, ESTIMATE, and CIBERSORT linked the 20 top CNGB3-associated genes to 24 immune lineages (Figure 5B). Samples were partitioned into CNGB3-high and -low groups by the median expression value, and the distribution of 22 immune-cell enrichment scores across these arms is depicted in Figure 5C. Associations between 24 immune cell types and CNGB3 are further illustrated by lollipop and chord plots in Figures 5E and 5F (ns, $p \geq 0.05$; *$p < 0.05$, **$p < 0.01$, ***$p < 0.001$).

3.5 Clinical and Prognostic Analysis

Correlations between CNGB3 and clinicopathologic features in TCGA-STAD are presented in Figures 6A-F, and six variables showed significant protein-level associations (Figures 6G-I). Kaplan-Meier analysis

revealed that OS, DSS, and PFI were markedly shorter among CNGB3-high patients (Figure 6J). A pan-cancer forest plot (Figure 6K) further suggests that CNGB3 may function as a broadly applicable survival-associated marker.

3.6 Prognostic Nomogram Model

Figure 7A presents univariate and multivariate Cox forest plots for OS. A nomogram forecasting 1-, 3-, and 5-year OS in gastric cancer is given in Figure 7B, alongside calibration curves at each landmark in Figure 7C. Full Cox regression results—including HR, 95% CI, and p values for every clinical covariate—are itemized in Tables 1 and 2.

Table 1. Univariate and Multivariate Cox Regression Analysis of Clinical Characteristics and CNGB3 Expression in Gastric Cancer Patients

Characteristic	N	Univariate Analysis	Univariate Analysis	Multivariate Analysis	Multivariate Analysis
		HR (95% CI)	p value	HR (95% CI)	p value
CNGB3	370				
Low	184	Reference		Reference	
High	186	1.464 (1.051 - 2.040)	0.024	1.297 (0.854 - 1.969)	0.223
Gender	370				
Female	133	Reference			
Male	237	1.267 (0.891 - 1.804)	0.188		
Age	367				
<= 65	163	Reference		Reference	
> 65	204	1.620 (1.154 - 2.276)	0.005	1.576 (1.052 - 2.359)	0.027
Pathologic T stage	362				
T1	18	Reference		Reference	
T2	78	6.725 (0.913 - 49.524)	0.061	20911605.248 (0.000 - inf)	0.995
T3	167	9.548 (1.326 - 68.748)	0.025	23380341.451 (0.000 - inf)	0.995
T4	99	9.634 (1.323 - 70.151)	0.025	25006236.239 (0.000 - inf)	0.995
Pathologic N stage	352				
N0	107	Reference		Reference	
N1	97	1.629 (1.001 - 2.649)	0.049	1.114 (0.505 - 2.457)	0.790
N2	74	1.655 (0.979 - 2.797)	0.060	1.417 (0.522 - 3.845)	0.494
N3	74	2.709 (1.669 - 4.396)	< 0.001	1.844 (0.701 - 4.849)	0.215
Pathologic M stage	352				
M0	327	Reference		Reference	

M1	25	2.254 (1.295 - 3.924)	0.004	0.880 (0.311 - 2.495)	0.810
Pathologic stage	347				
Stage I	50	Reference		Reference	
Stage II	110	1.551 (0.782 - 3.078)	0.209	1.455 (0.421 - 5.026)	0.553
Stage III	149	2.381 (1.256 - 4.515)	0.008	1.183 (0.241 - 5.810)	0.836
Stage IV	38	3.991 (1.944 - 8.192)	< 0.001	2.060 (0.355 - 11.951)	0.420
Primary therapy outcome	313				
PD	64	Reference		Reference	
SD	16	0.590 (0.267 - 1.305)	0.193	0.769 (0.314 - 1.881)	0.565
PR	4	0.750 (0.233 - 2.412)	0.629	0.622 (0.176 - 2.190)	0.459
CR	229	0.215 (0.145 - 0.319)	< 0.001	0.268 (0.173 - 0.414)	< 0.001
Histologic grade	361				
G1	10	Reference			
G2	134	1.648 (0.400 - 6.787)	0.489		
G3	217	2.174 (0.535 - 8.832)	0.278		
H pylori infection	162				
No	144	Reference			
Yes	18	0.650 (0.279 - 1.513)	0.317		

Abbreviations: HR = Hazard Ratio; CI = Confidence Interval. Statistically significant p values (< 0.05) are shown in bold.

Table 2. Variable Selection for Multivariate Cox Regression Model

Variable	Univariate p (worst level)	Entered Multivariate Model	Multivariate p (worst level)
CNGB3	0.024	Yes	0.223
Gender	0.188	No (p > 0.05)	-
Age	0.005	Yes	0.027
Pathologic T stage	0.025 (T3/T4)	Yes	0.995*
Pathologic N stage	< 0.001 (N3)	Yes	0.215 (N3)
Pathologic M stage	0.004	Yes	0.810
Pathologic stage	< 0.001 (Stage IV)	Yes	0.420 (Stage IV)
Primary therapy outcome	< 0.001 (CR)	Yes	< 0.001 (CR)
Histologic grade	0.278 (G3)	No (p > 0.05)	-
H. pylori infection	0.317	No (p > 0.05)	-

* Pathologic T stage showed inflated HR and CI in multivariate analysis due to small subgroup size (T1: n = 18).

4. Discussion

Gastric cancer carries a sobering prognosis; early symptoms are frequently subtle, recurrence and dissemination are common, and resistance to conventional therapy is a recurring problem [6]. The disease is markedly heterogeneous, and treatment responses differ considerably between individuals [7]. A nationwide Chinese analysis of 220,304 patients treated at 53 major centers across 27 provinces reported 1-, 2-, 3-, 4-, and 5-year survival of 74.07%, 54.89%, 44.21%, 37.97%, and 33.53%, respectively [8]. High-throughput sequencing, proteomics, and metabolomics have illuminated recurrent genetic lesions and biological processes in this disease, and molecular clustering has stratified gastric cancer into subtypes amenable to tailored interventions [9]. Notably, the tumor-reprogrammed pulmonary immune environment profoundly shapes the behavior of tissue-resident immune cells, and tissue-resident macrophages can acquire enhanced anti-tumor activity within such an altered microenvironment [14].

The present work centers on CNGB3, a molecule implicated in gastric cancer cell growth, motility, and spread. Prior investigations have documented dysregulated CNGB3 across diverse malignancies, with gastric cancer among the most prominent, where its expression tracks tumor aggressiveness and outcome [3]. By integrating differential-expression, functional-enrichment, and immune-infiltration analyses, we aim to clarify the mechanistic and translational implications of CNGB3 in gastric cancer.

Consistent with the transcriptomic findings, CNGB3 was strongly upregulated in gastric tumor tissue relative to normal mucosa. GEO-based analysis additionally demonstrated that CNGB3 rose further in

metastatic gastric cancer, underscoring a plausible contribution to dissemination. GSEA confirmed significant enrichment of CNGB3 across other tumor entities ($p < 0.05$) [10], reinforcing its pan-cancer significance.

With respect to immunity, notable differences in immune-cell infiltration separated the CNGB3-high and CNGB3-low groups. The observed elevations in activated NK cells and CD8+ T cells hint that CNGB3 may facilitate immune evasion by reshaping the tumor microenvironment, and raise the possibility that it could be exploited in immunotherapy, especially together with immune checkpoint blockade. CNGB3 therefore merits consideration as a therapeutic target in gastric cancer.

Immunohistochemistry confirmed that CNGB3 protein is appreciably elevated in gastric cancer relative to adjacent non-neoplastic tissue, reinforcing its biological relevance. Differential-expression analysis identified 2,059 DEGs and 20 hub genes, and the assembled PPI network provides a platform for future functional studies of CNGB3. In parallel, a proteomic-immunologic model of postoperative peritoneal metastasis in gastric cancer underscores the interplay between protein-level and immune determinants [11].

Kaplan-Meier analysis showed that patients with high CNGB3 expression had significantly poorer OS, DSS, and PFS than those with low expression (all $p < 0.05$). These data identify elevated CNGB3 as an adverse prognostic indicator and support its utility as a biomarker. Integration with additional clinical covariates in future work will help consolidate its prognostic value.

Collectively, these observations position CNGB3 as both a prognostic biomarker and a candidate therapeutic target. Its link to immune-cell infiltration implies that CNGB3 may remodel the tumor microenvironment to foster immune evasion and more aggressive disease. This dual function in tumor advancement and immune regulation warrants continued clinical investigation.

Several limitations should be acknowledged. First, the lack of experimental validation in wet-lab models tempers the causal inferences drawn here. Second, because the analyses depend on publicly archived datasets (TCGA, GEO), the results carry the selection bias inherent to retrospective data. Third, without multicenter confirmation, the generalizability of our conclusions remains constrained. Larger, prospective cohorts and functional experiments will be required to strengthen the translational relevance of these findings.

5. Conclusion

This study establishes CNGB3 as a meaningful biomarker and prognostic indicator in gastric cancer. The results illuminate its influence on tumor cell behavior, its ties to immune infiltration, and its association with adverse outcome, advancing prospects for early detection and personalized treatment. Although wet-lab validation and multicenter studies are still needed, continued investigation of CNGB3 may eventually translate into more effective strategies for gastric cancer management.

Declarations

Author Contributions

Hangying Lin: Data curation (equal); formal analysis (equal); investigation (equal); project administration (equal); writing – original draft (lead). Zhirong Yang: Data curation (equal); formal analysis (equal); project administration (equal); writing – original draft (equal). Shangzhe Zheng: Data curation (equal); project administration (equal). Yun Lin: Data curation (equal).

Acknowledgments

The authors greatly thank Zhirong Yang and Xi Chen for their support.

Conflict of Interest Statement

The authors have no conflict of interest.

Data Availability Statement

The datasets analyzed during this study are publicly available in the following repositories and are cited by their precise project identifiers: The Cancer Genome Atlas Stomach Adenocarcinoma cohort (TCGA-STAD); the Genotype-Tissue Expression project (GTEx); the Gene Expression Omnibus dataset GSE84437; the Clinical Proteomic Tumor Analysis Consortium proteomic resource (CPTAC), accessed via the UALCAN portal; and the Human Protein Atlas (HPA). All source records can be retrieved directly from the respective repositories using these identifiers. Analytical code is available from the corresponding author upon reasonable request.

Funding Information

This study was supported by the Natural Science Foundation of Fujian Province (Grant No. 2024J011162).

Ethics Statement

This study did not involve animal experiments; therefore, Institutional Animal Care and Use Committee (IACUC) approval was not required. All human data were obtained from publicly available, de-identified databases (TCGA, GTEx, GEO, CPTAC, Human Protein Atlas), and no prospective patient samples or identifiable human subjects were used; thus, Institutional Review Board (IRB) approval and informed consent were not required.

□□□□□□□□□□□□

Publication Consent

Publication Consent: All authors have read and approved the final manuscript and consent to its publication in Discover Oncology. This study reports no individual patient data, images, or other identifiable information; therefore, no separate individual publication consent was required.

References

1. Sundar R, Nakayama I, Markar SR, et al. Gastric cancer. Lancet, 2025, 405(10494): 2087-2102. doi: 10.1016/S0140-6736(25)00725-6
2. Tan J, Zhao D, Wang Q, et al. Whole exome sequencing study identifies distinct characteristics of transformed small cell lung cancer with EGFR mutation compared to de novo small cell and primary non-small cell lung cancers. Cancer Med, 2025, 14(7): e70838. doi: 10.1002/cam4.70838
3. Chen S, Wang Z. Integration of multi-omics and nucleotide metabolism reprogramming signature analysis reveals gastric cancer immunological and prognostic features. Cancer Cell Int, 2024, 24(1): 212. doi: 10.1186/s12935-024-03369-7
4. Matsuoka T, Yashiro M. Bioinformatics analysis and validation of potential markers associated with prediction and prognosis of gastric cancer. Int J Mol Sci, 2024, 25(11): 5880. doi: 10.3390/ijms25115880
5. Uhlen M, Fagerberg L, Hallstrom BM, et al. Proteomics. Tissue-based map of the human proteome. Science, 2015, 347(6220): 1260419. doi: 10.1126/science.1260419
6. Hu M, Tao P, Wang Y, et al. Knockdown of CCNB2 inhibits the tumorigenesis of gastric cancer by regulation of the PI3K/AKT pathway. Sci Rep, 2025, 15(1): 5703. doi: 10.1038/s41598-025-88981-1
7. Hu Y, Wang B, Shi C, et al. A machine learning approach to risk-stratification of gastric cancer based on tumour-infiltrating immune cell profiles. Ann Med, 2025, 57(1): 2489007. doi: 10.1080/07853890.2025.2489007
8. Chen Y, Jia K, Xie Y, et al. The current landscape of gastric cancer and gastroesophageal junction cancer diagnosis and treatment in China: A comprehensive nationwide cohort analysis. J Hematol Oncol, 2025, 18(1): 42. doi: 10.1186/s13045-025-01612-8
9. Ma Y, Jiang Z, Pan L, et al. Current development of molecular classifications of gastric cancer based on omics (Review). Int J Oncol, 2024, 65(3): 99. doi: 10.3892/ijo.2024.5675
10. Huang D, Li J, He Z, et al. Pan-cancer and experimental analyses reveal the immunotherapeutic significance of CST2 and its association with stomach adenocarcinoma proliferation and metastasis. Front Immunol, 2024, 15: 1466806. doi: 10.3389/fimmu.2024.1466806
11. Li X, Lu J, Chen F, et al. Comprehensive proteomic analysis and multidimensional model construction of peritoneal metastasis in gastric cancer. Cancer Lett, 2025, 614: 217509. doi: 10.1016/j.canlet.2025.217509

12. Alom S, Anal B, Ghosh S. Recently Emerging Liquid Biopsy-based Non-invasive Methylation Biomarkers for Gastric Cancer Diagnosis, Prognosis and Therapy Response Prediction. Curr Cancer Ther Rev, 2025, 21(2). doi: 10.2174/0115733947313656240819093316
13. Moayyedkazemi A, Azadbakht S, Baharvand P, Saki M. Gastric Cancer: A Review of Risk Factors and New Insights into Treatment. Curr Cancer Ther Rev, 2023, 19(2): 85-96. doi: 10.2174/1573394718666220428105301
14. Ren M, Dou J, Yue Q, Ma L, Yu H, Shang S, et al. Alveolar macrophages maintain tissue localization and gain enhanced anti-tumor activity in Lewis lung carcinoma-reprogrammed lung microenvironment. Front Immunol, 2025, 16: 1616514. doi: 10.3389/fimmu.2025.1616514

Figures

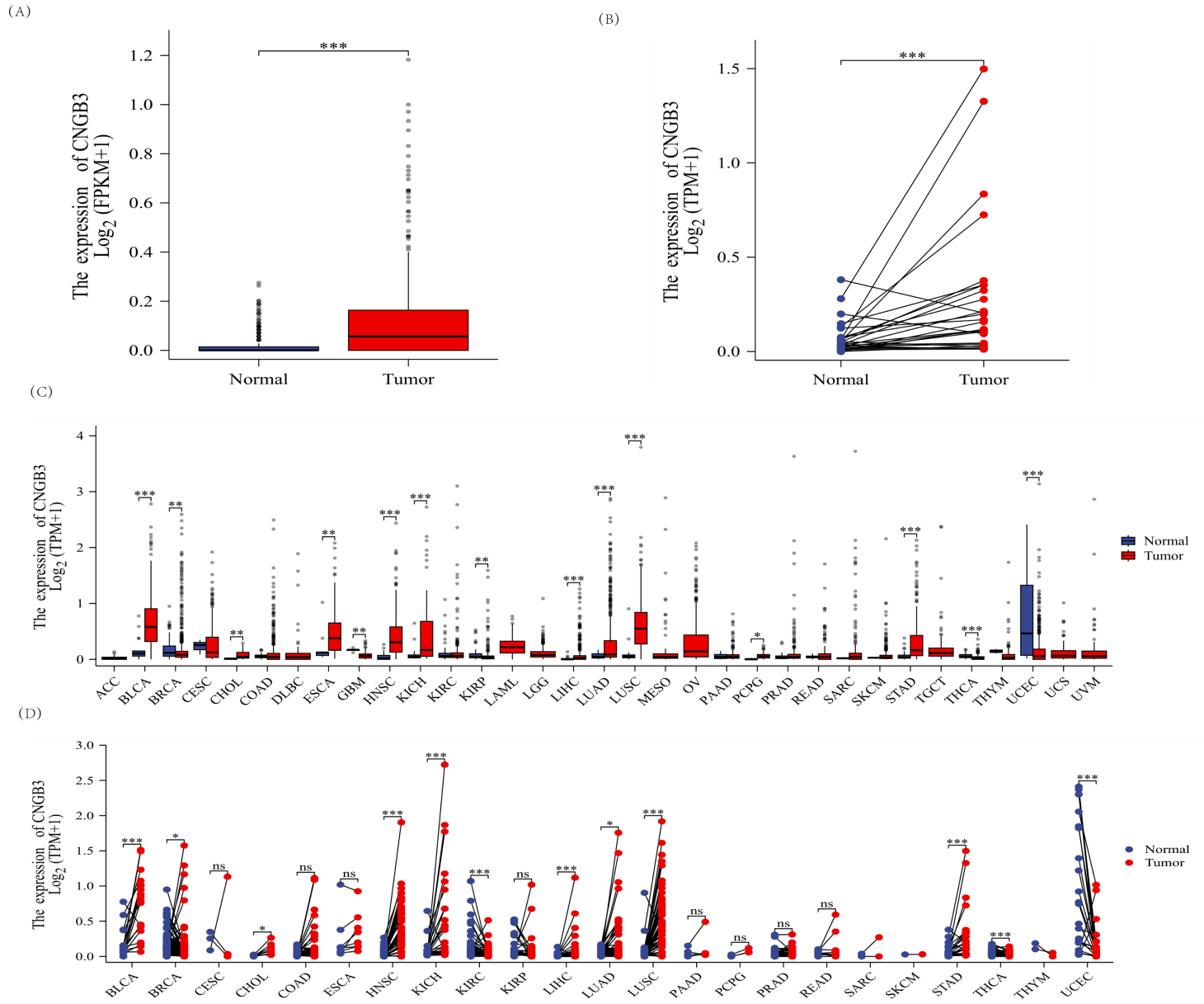


Figure 1

CNGB3 expression in gastric cancer and pan-cancer analysis. (A) CNGB3 expression in STAD tumor vs. normal tissues from TCGA; (B) CNGB3 expression in paired STAD samples; (C) Pan-cancer expression of CNGB3 across 33 cancer types in TCGA+GTEx; (D) CNGB3 expression in paired samples across multiple cancer types.

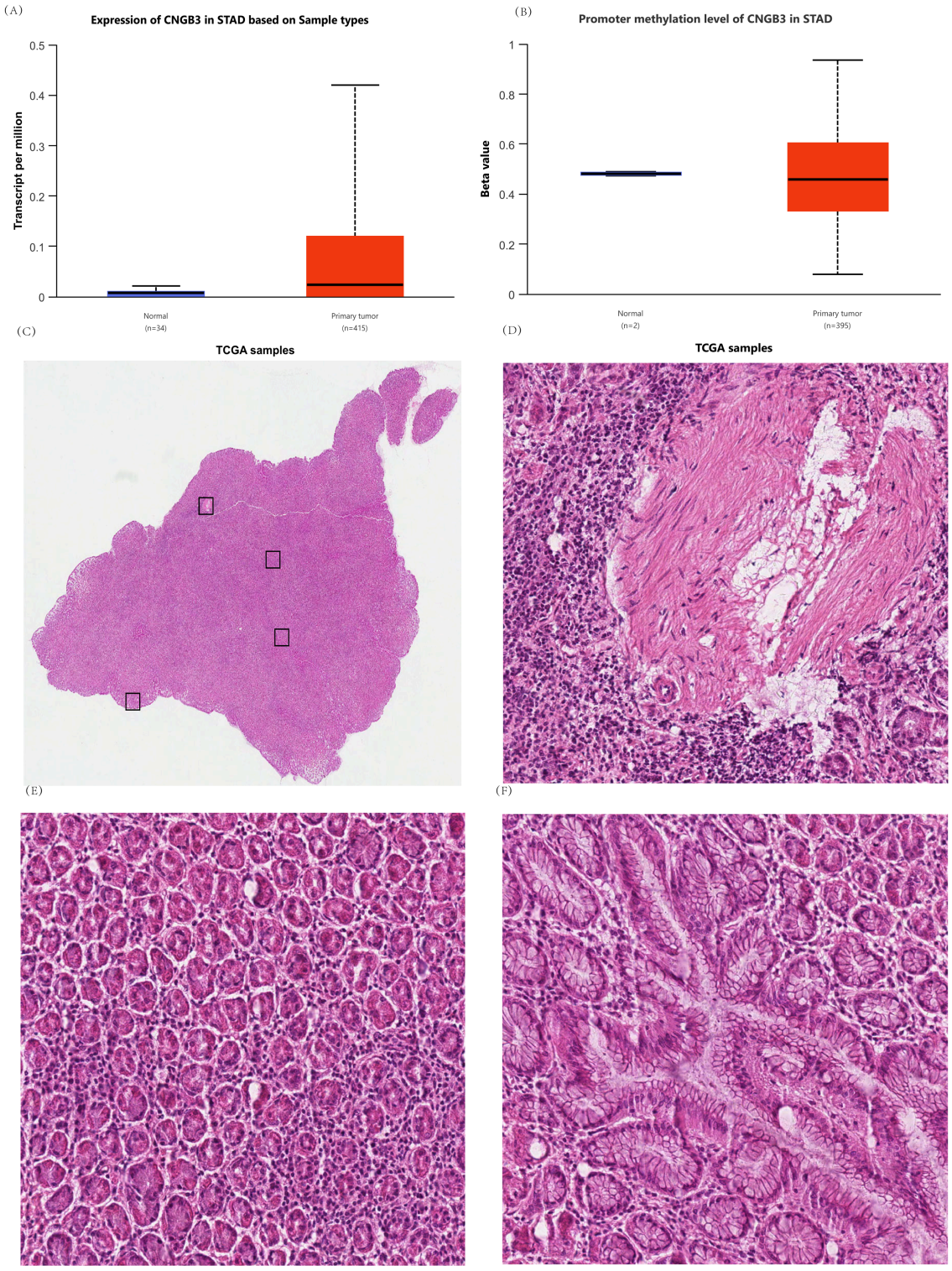


Figure 2

CNGB3 protein expression, methylation, and immunohistochemical validation. (A) CNGB3 protein expression (CPTAC); (B) Promoter methylation levels; (C-D) IHC staining of CNGB3 in normal vs. tumor tissues; (E-F) Representative IHC images from the Human Protein Atlas.

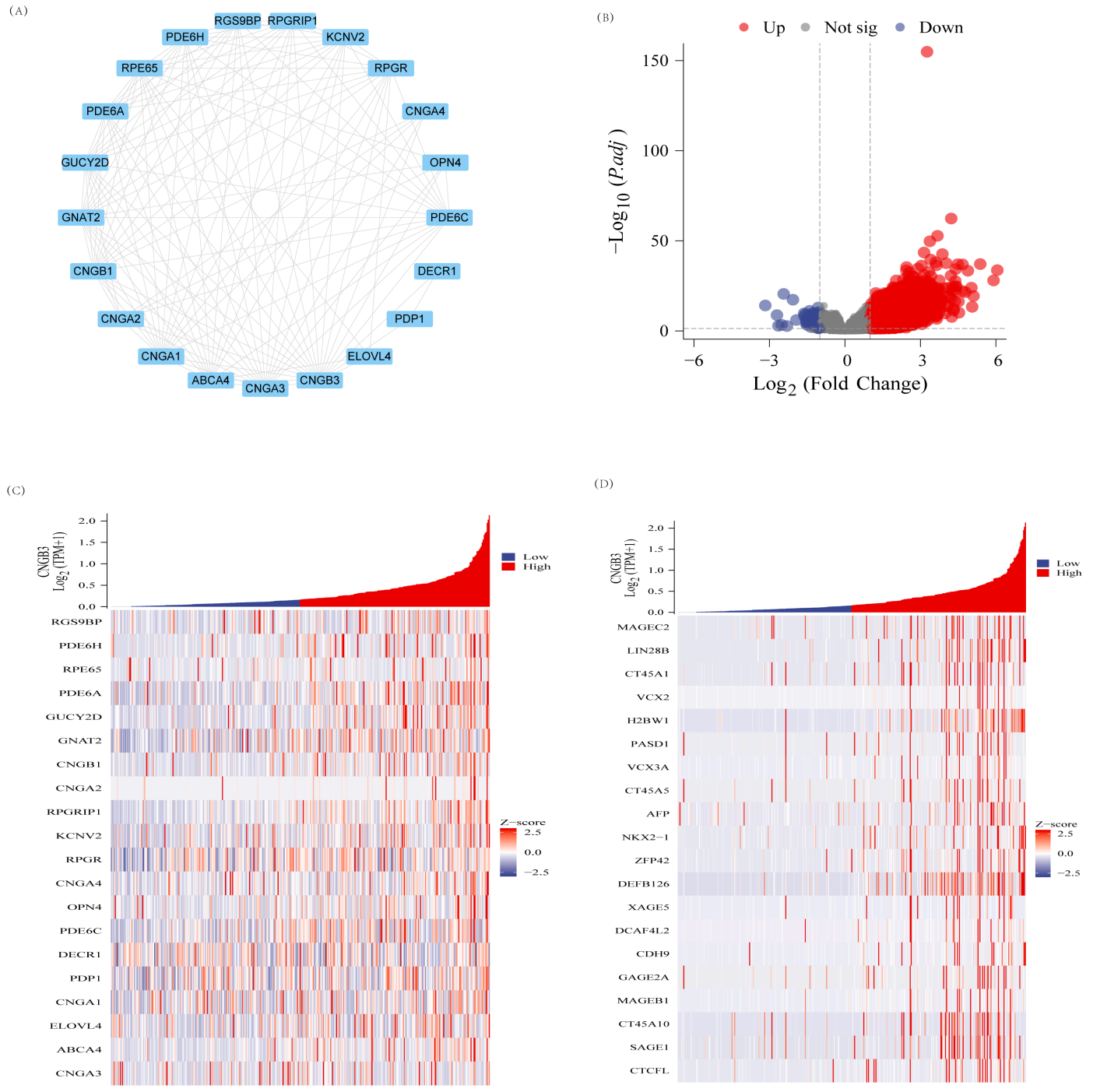


Figure 3

Differential expression and co-expression analysis of CNGB3. (A) PPI network of 20 hub genes; (B) Volcano plot of DEGs; (C) Heatmap of hub gene expression; (D) Co-expression correlation heatmap of top 20 CNGB3-associated genes.

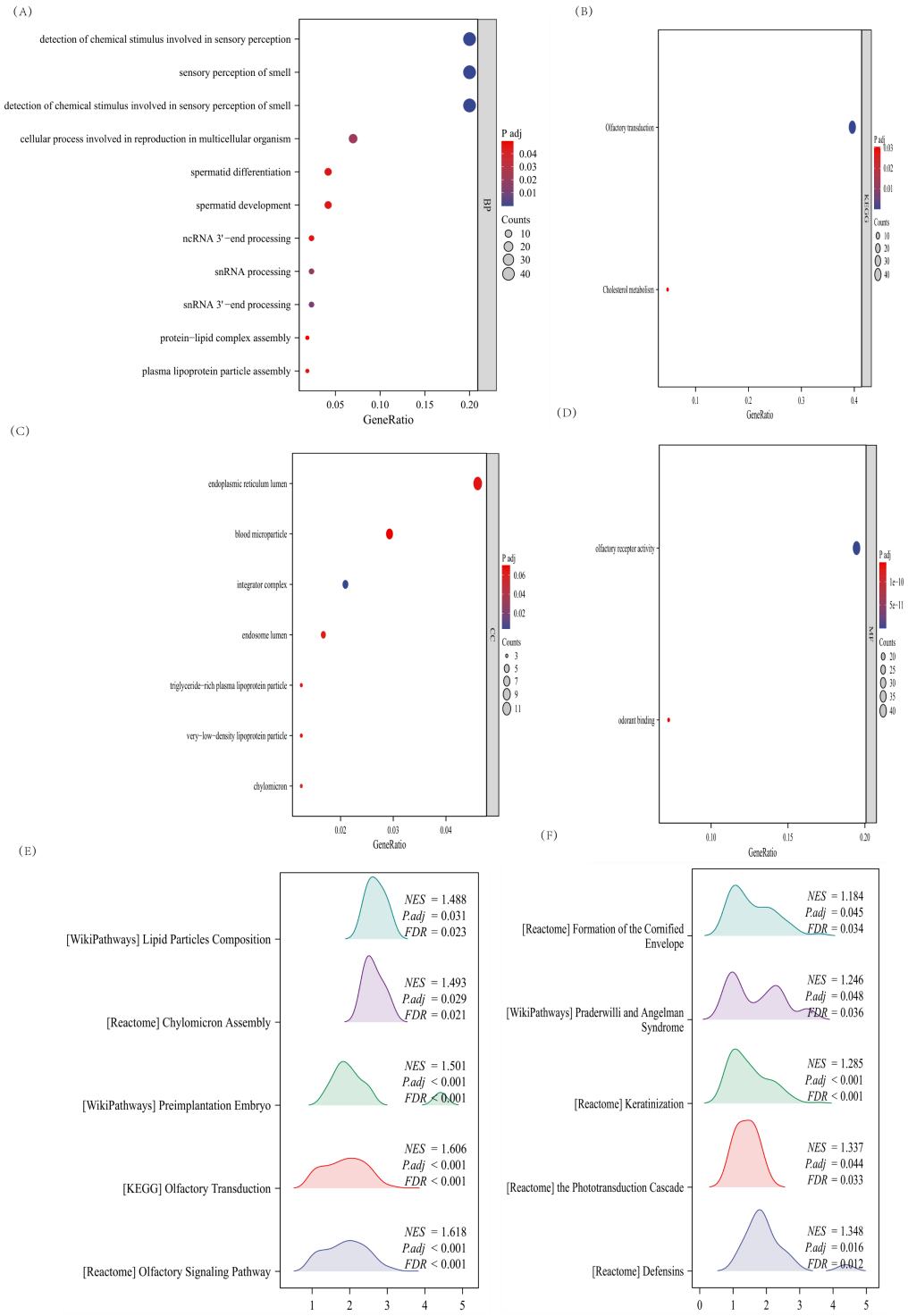


Figure 4

GO and GSEA functional enrichment analysis. (A-D) GO enrichment analysis (BP, CC, MF, and KEGG pathways); (E-F) GSEA enrichment plots showing significantly enriched pathways (EMT, oxidative phosphorylation, allograft rejection, inflammatory response, fatty acid metabolism).

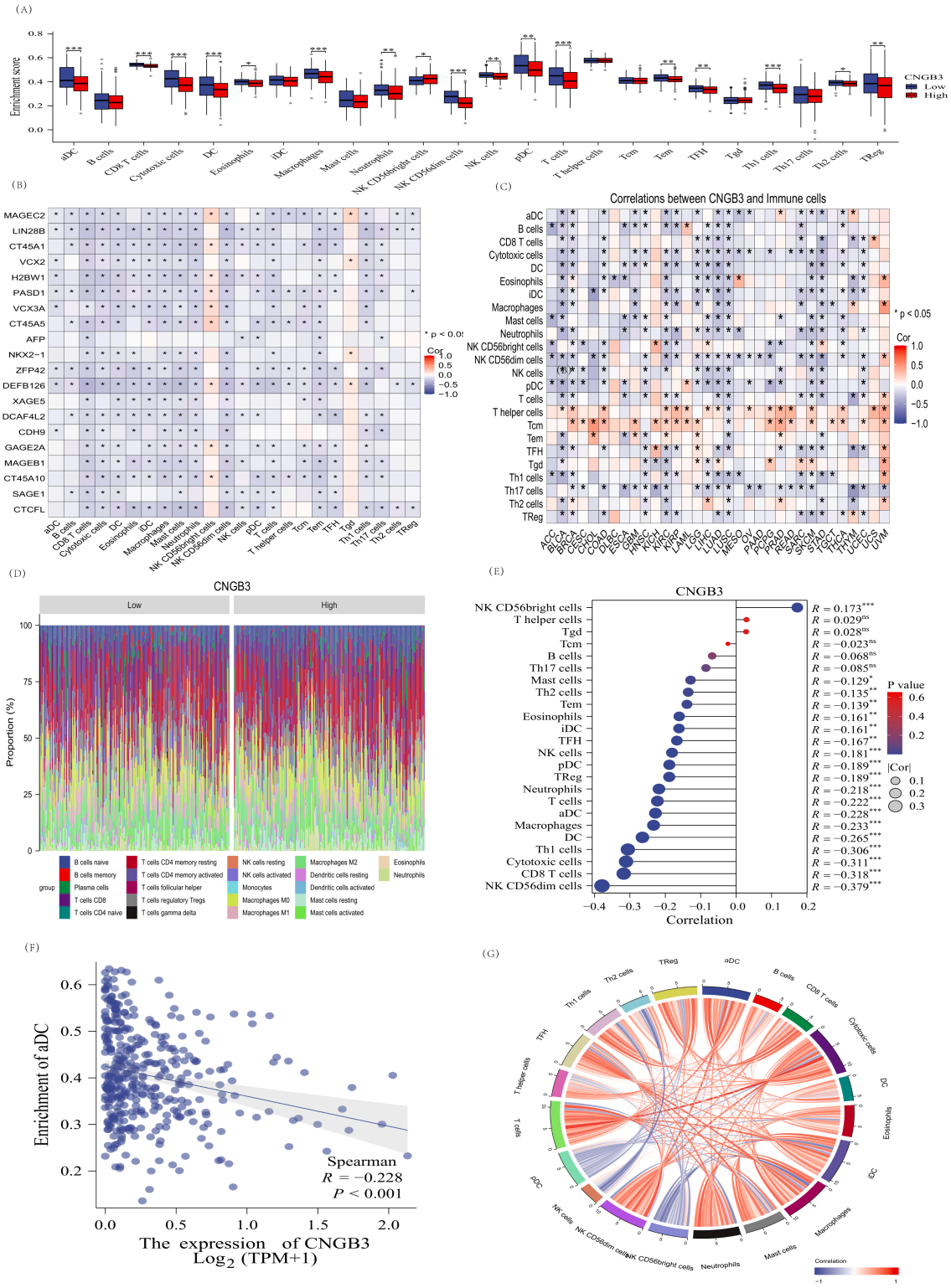


Figure 5

Immune infiltration analysis. (A) Enrichment scores of 24 immune cell types between CNGB3-high and CNGB3-low groups; (B) Correlation heatmap of hub genes and immune cells; (C) Distribution of 22 immune cell types by CNGB3 expression groups; (D) Immune cell composition stacked bar chart; (E) Lollipop plot of CNGB3-immune cell correlations; (F-G) Scatter plots of CNGB3 expression vs. key immune cells (aDC, TReg, Th2, B cells, CD8 T cells, Cytotoxic cells).

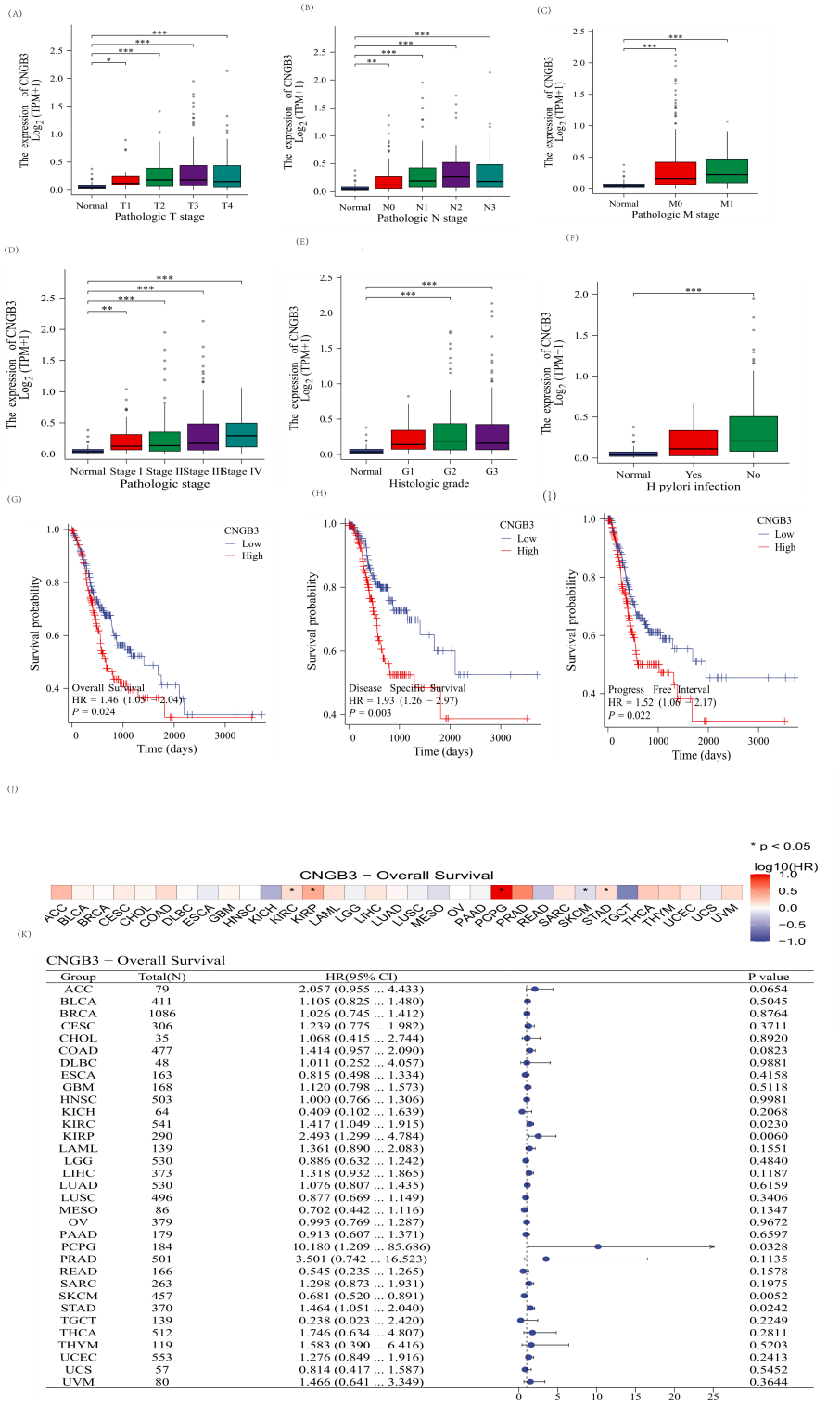


Figure 6

Clinical correlation and survival analysis. (A-F) CNGB3 expression across clinicopathological variables (T stage, N stage, M stage, pathologic stage, histologic grade, H. pylori infection); (G-I) Kaplan-Meier survival curves for OS, DSS, and PFI; (J) Pan-cancer forest plot of CNGB3 prognostic significance; (K) Detailed forest plot of CNGB3 OS hazard ratios across 33 cancer types.

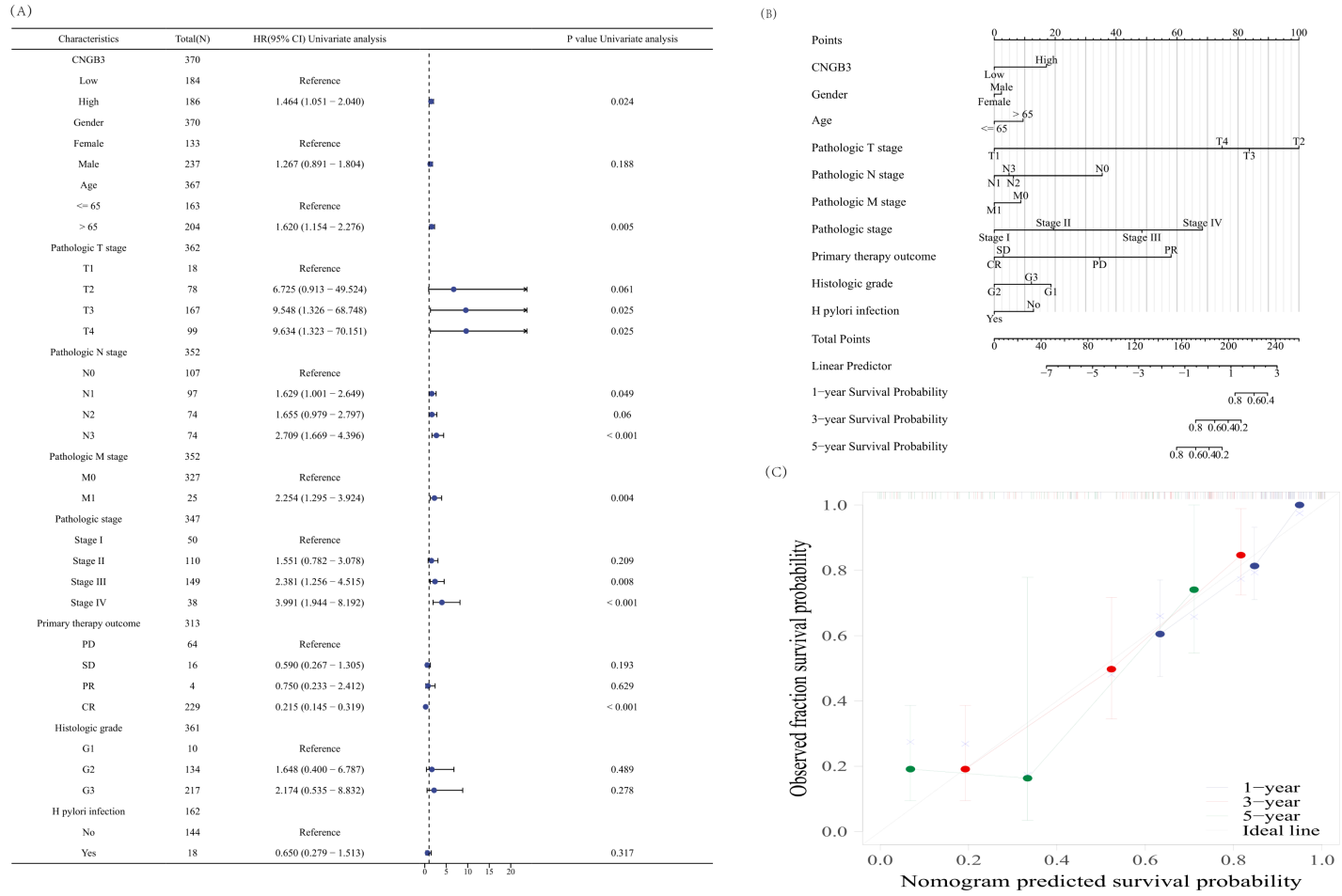


Figure 7

Prognostic nomogram and calibration. (A) Forest plot of univariate Cox regression analysis for OS; (B) Nomogram predicting 1-, 3-, and 5-year OS in gastric cancer patients; (C) Calibration curves for the nomogram at 1, 3, and 5 years.

Supplementary Files

This is a list of supplementary files associated with this preprint. Click to download.

- GraphicalAbstract.docx
- Supplementary.docx